Electronic Structure and Magnetic Properties of Iridate Superlattice $SrIrO_3/SrTiO_3$

Kang-Hwan Kim[1*], Heung-Sik Kim[1*], and Myung Joon Han[1,2]
[1] *Department of Physics, Korea Advanced Institute of Science and Technology, Daejeon, 305-701, Korea and*
[1] *KAIST Institute of NanoCentury, Korea Advanced Institute of Science and Technology, Daejeon, 305-701, Korea**

Motivated by an experimental report of iridate superlattices, we performed first-principle electronic structure calculations for $SrIrO_3/SrTiO_3$. Heterostructuring causes $SrIrO_3$ to become Sr_2IrO_4-like, and the system has the well-defined $j_{\rm eff} = 1/2$ states near the Fermi level as well as canted antiferromagnetic order within the quasi-two-dimensional IrO_2 plane. In response to a larger tensile strain, the band gap is increased due to the resulting increase in bond length and the bandwidth reduction. The ground state magnetic properties are discussed in comparison to the metastable collinear antiferromagnetic state. Our work sheds new light for understanding the recent experimental results on the iridate heterostructures.

arXiv:1402.2503v1 [cond-mat.str-el] 11 Feb 2014

I. INTRODUCTION

Recently atomic spin-orbit coupling (SOC) has become a central issue in condensed matter physics[1–3]. In strong SOC, spin and orbital degrees of freedom are entangled, and this characteristic often plays a key role in the emergence of new material properties. Iridium oxide compounds are of special interest due to the fact that other atomic energy scales, such as U and J, happen to be in a size comparable to SOC in this class of materials. Owing to the cooperation between those energy scales, novel low-energy states, designated by $j_{\rm eff}$ (the effective total angular momentum)[4,5], and exotic quantum ground states can be realized[6–9].

The Ruddlesden-Popper (RP) series of iridates, $Sr_{n+1}Ir_nO_{3n+1}$, are known to exhibit quite different features depending on n. Ideally, by making the lower dimensional forms, one can change and even control their properties. Several recent reports on the iridate thin films[10–13] provide a good playground for investigation from this perspective. Also, $SrIrO_3/SrTiO_3$ (SIO/STO) superlattice (SL) seems to have been synthesized successfully[14]. According to the recent report by Matsuno *et al.*, controlled and systematic changes are found in $[SIO]_m/[STO]_1$ as a function of SIO layer thickness, m. These experiments open a new stage in the study of iridate physics by enabling control of their dimensionality and therefore of their material characteristics.

One of the most interesting questions in these SLs may be how close the thinnest SL can be to Sr_2IrO_4 because SIO and Sr_2IrO_4 are the two end members of the RP series. If the property of m=1 SL is similar to those of Sr_2IrO_4, the physics of the whole RP series can in principle be accessed in the SL by changing SIO thickness. Further, epitaxial strain provides an extra dimension for controlling their properties.

With this motivation, we performed density functional theory calculations for this SIO/STO. It was found that this form of SL actually exhibits quite similar characteristics to Sr_2IrO_4 and is notably different from the other RP iridates, such as $Sr_3Ir_2O_7$. It has an insulating ground state and canted antiferromagnetic (AF) ordering of $j_{\rm eff} = 1/2$ moments. The electronic and magnetic properties are systematically changed by strain. Our results shed new light for understanding the novel correlated spin-orbital physics of iridate compounds.

II. COMPUTATIONAL DETAILS

First-principles electronic structure calculations were performed by OPENMX code[15,16], which is based on the linear combination of pseudoatomic orbitals method[17]. The Perdew-Burke-Ernzerhof (PBE) exchange-correlation functional[18] was adopted. The energy cutoff of 300 Ry and the Monkhorst-Pack k-meshes of $7 \times 7 \times 5$ in the first Brillouin zone were used for the real and momentum space integrations, respectively. SOC was treated within a fully relativistic j-dependent pseudopotential scheme in the non-collinear methodology[16]. Electronic correlations were taken into account with the DFT+U formalism[19]. We used the effective on-site Coulomb interaction parameter of $U_{\rm eff} \equiv U - J = 2.0$ eV for the Ir $5d$ orbitals[20,21]. The optimized c-axis lattice constant and the internal coordinates are compared well with the result by Vienna *ab-initio* Simulation Package[22,23]. The energy criteria was 10^{-3} eV for the structural optimization.

* These two authors contributed equally.

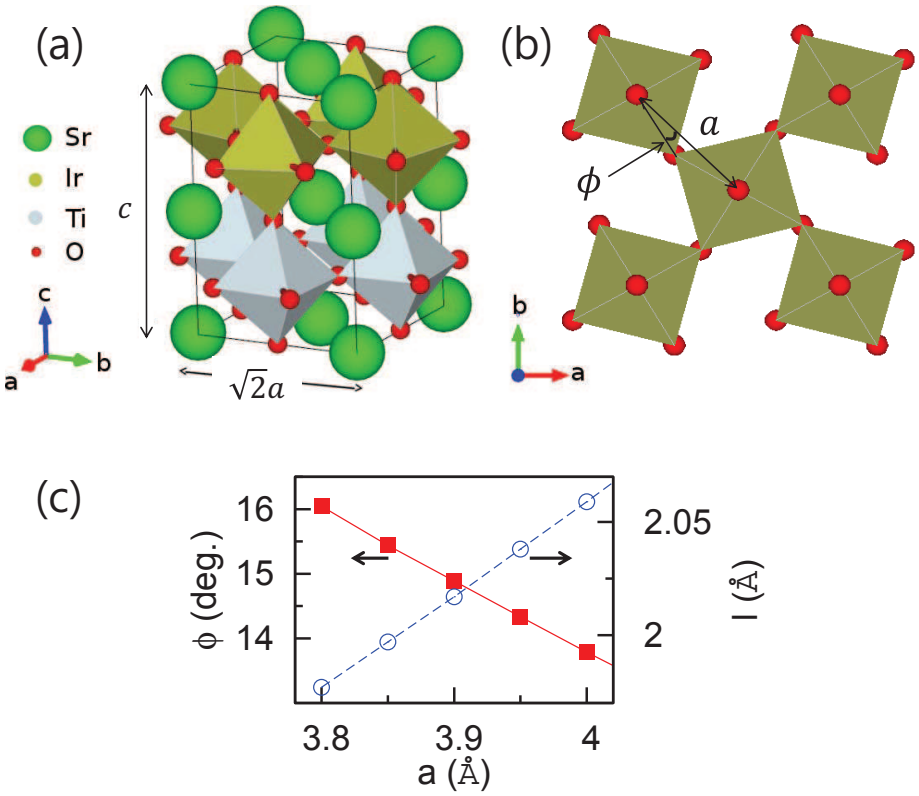

FIG. 1: (a) The unicell structure used in this study. (b) Top view of the optimized geometry of IrO_6 cages where a and ϕ refer to the distance between the nearest Ir atoms and the Ir-O-Ir bond angle, respectively. (c) The calculated structure parameters as a function of in-plain lattice constants, a. ϕ and l denote the octahedral rotation angle and the Ir-O bond length, respectively.

III. RESULTS AND DISCUSSION

A. Structural properties

Fig. 1(a) shows the unitcell structure used in this study. As in Sr_2IrO_4, this SL has TiO_2 inter-layers which are electronically inactive (d^0 configuration) and effectively suppress hopping between the neighboring IrO_2 layers. Therefore our system becomes quasi-two-dimensional, as is the case in Sr_2IrO_4. It was also found that the larger IrO_6 octahedra have antidistortive rotations along the c-axis in order to fit into the smaller SrO_6 cage (with the rotation angle ϕ) as depicted in Fig. 1(b). This produces an environment for the electronic behavior similar to the Ir ions in Sr_2IrO_4.

To simulate the epitaxial strain, the in-plain lattice constants were varied from 3.80 to 4.00Å. Note that the equilibrium in-plane lattice constant of Sr_2IrO_4 is ∼3.88 Å [11,24]. If we assume the IrO_6 octahedra are rigid (*i.e.,* no change in the Ir-O bond lengths), it is natural to expect the enhancement (reduction) of the octahedral rotation for the compressive (tensile) strain. In fact, our result qualitatively follows such a tendency in the rotation pattern. Simultaneously, however, we also found that the IrO_6 octahedra undergo significant tetragonal distortions, as summarized in Fig. 1(c). The in-plane Ir-O bond length is changed by $\sim \pm 2.0\%$ as a is increased from 3.90 Å to 4.00 Å(tensile strain) or decreased down to 3.80 Å(compressive strain).

B. Electronic properties without $U_{\rm eff}$

Fig. 2 presents the calculated band structure with SOC ($U_{\rm eff}$=0). The size and color of each band point represents the portions of t_{2g} and $j_{\rm eff}$ states, respectively. As expected, the t_{2g} characters prevail around the Fermi energy. The threefold degenerate t_{2g} states carry the effective orbital angular momentum $l_{\rm eff} = 1$. Assuming that the SOC of the Ir atom dominates over the other energy scales, such as bandwidths and tetragonal crystal fields, the $(l_{\rm eff} = 1)\oplus(s = 1/2)$ states are split into an upper $j_{\rm eff}$=1/2 doublet and a lower $j_{\rm eff}$=3/2 quartet[4], where the $j_{\rm eff} = 1/2$ and 3/2 states are

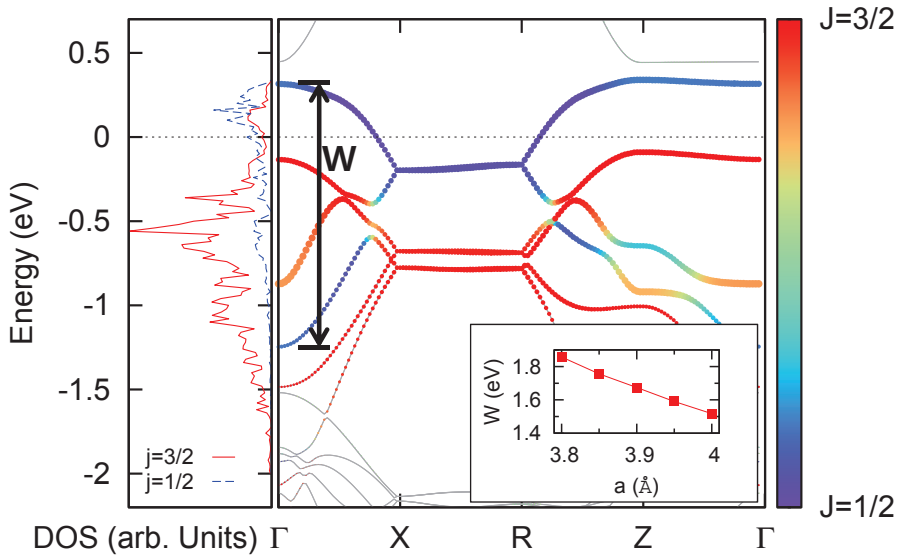

FIG. 2: The calculated band structure with SOC ($U_{\rm eff}$=0 and with a=3.95 Å). The size and color of the point represent the amount of t_{2g} and $j_{\rm eff}$-character, respectively. (Inset) The dependence of the calculated bandwidths on the in-plain lattice constant.

defined as

$$
\begin{aligned}
|j_{\rm eff}=\frac{1}{2},\pm\frac{1}{2}\rangle_z &\equiv \mp\sqrt{\frac{1}{3}}|d_{xy}\rangle|\uparrow\downarrow\rangle_z \mp \sqrt{\frac{2}{3}}\left[\frac{\pm|d_{yz}\rangle+i|d_{xz}\rangle}{\sqrt{2}}\right]|\downarrow\uparrow\rangle_z \\
&\equiv \pm\sqrt{\frac{1}{3}}|0,\uparrow\downarrow\rangle_z \mp \sqrt{\frac{2}{3}}|\pm 1,\downarrow\uparrow\rangle_z \\
|j_{\rm eff}=\frac{3}{2},\pm\frac{1}{2}\rangle_z &\equiv \sqrt{\frac{2}{3}}|0,\uparrow\downarrow\rangle_z + \sqrt{\frac{1}{3}}|\pm 1,\downarrow\uparrow\rangle_z \\
|j_{\rm eff}=\frac{3}{2},\pm\frac{3}{2}\rangle_z &\equiv |\pm 1,\uparrow\downarrow\rangle_z
\end{aligned}
\tag{1}
$$

where $\{\uparrow,\downarrow\}$ and $\{0,\pm1\}$ denote the indices for the spin and the angular momentum eigenstates $|s=1/2;\pm1/2\rangle_z$ and $|l_{\rm eff}=1;0,\pm1\rangle_z$, respectively, and the subscript z means that the momenta are quantized along the octahedral z-direction (perpendicular to the Ir plane). Although the splitting between the $j_{\rm eff}=1/2$ and 3/2 states is not perfect due to the sizeable effect from the bandwidth and the confinement in the SL, the $j_{\rm eff}=1/2$ characters in the low-energy states near the Fermi level are quite clearly noticed (blue colors in Fig. 2). It is found that the $j_{\rm eff}$-characterization of the bands is valid in the whole range of strains we considered in this study. There are some minor differences between the band structure of SL in Fig. 2 and the bulk Sr_2IrO_4: In Fig. 2, the position of the valence band top at X point is lower by ∼0.1eV than that at Γ, while they are nearly at the same energy in Sr_2IrO_4[4,25]. The same feature is also observed in the $U>0$ calculations (Fig. 3(a)). The presence of the additional tetragonal crystal field, induced by the interface effect and the strain, yields some small changes in the relative position of the $j_{\rm eff}$=1/2 and 3/2 bands compared to the bulk Sr_2IrO_4.

The bandwidth W of the low-energy $j_{\rm eff}$=1/2 states, which are located near the Fermi level, is of key importance in understanding the electronic property of RP iridates[26]. One way of defining W is at the Γ point as shown in Fig. 2. The inset of Fig. 2 presents the change of W as a function of strain. It is clearly seen that the bandwidth W is decreased as larger tensile strain is applied. This result can be surprising if one tries to understand the system based on the 'rigid IrO_6 octahedron' picture (see, for example, the discussion in Nichols *et al.*[11]). It is therefore important to note that the Ir-O bond lengths are increased (decreased) under tensile (compressive) strain as mentioned above. Since enlarged bond lengths generally reduce hopping, the reduction of the bandwidth by the tensile strain is attributed to the bond length changes.

C. Electronic and magnetic properties with $U_{\rm eff}$

Fig. 3(a)-(d) summarizes the calculation results with SOC and $U_{\rm eff}$=2 eV. Two different magnetic configurations have been considered; the canted AF spin order (the ground state configuration of Sr_2IrO_4; see the inset of Fig. 3(a)) and the collinear AF order (the ground state of $Sr_3Ir_2I_7$; see the inset of Fig. 3(b)). In the canted AF state, the Ir moments lie within the *ab*-plane and their angles follow the tilting angles of IrO_6 octahedra. In the collinear AF state, the moments are parallel to the c-axis. It is found that, as in Sr_2IrO_4, the canted AF state is more stable than the collinear AF state by about 3 meV/Ir over the strain range considered in this study.

In both magnetic configurations, the electronic correlation is found to play the key role in opening the gap and stabilizing the AF order as well as the dominant $j_{\rm eff}$=1/2 character in the upper Hubbard bands. Similar features were also observed in the previous study of Sr_2IrO_4[27]. The calculated band gap of the canted and the collinear AF phase at $a = 3.90$Å , 0.35 and 0.31 eV, respectively, is comparable to the optical gap of ∼0.5 for Sr_2IrO_4 bulk and thin films[11,26], considering a little ambiguity in the $U_{\rm eff}$ parameter. Note that, when a larger (tensile) strain is applied, the band gap is markedly increased as shown in Fig. 3(c), which is consistent with the decreasing trend of W (see Fig. 2). Importantly, this trend is in a good agreement with recent optical spectroscopy data by Nichols *et al.* for the Sr_2IrO_4 thin film under various strain conditions in which the enhancement of the optical gap upon tensile strain was observed[11]. This feature is hard to understand from the point of view of the conventional rigid IrO_6 picture as discussed in Nichols *et al.*[11], whereas our result based on the tetragonal distortion of the IrO_6 octahedra provides a natural explanation.

Although the collinear AF phase is less stable than the canted AF, the data from this configuration also provides useful information. First, we note that the gap size in the collinear AF is smaller than that of the canted AF state over the entire range of strain. It is interesting to note that the gap is closed at $a = 3.80$Å and the spin moment vanishes simultaneously. Since $[SIO]_1/[STO]_1$ SL has considerable similarities in the electronic and magnetic properties with Sr_2IrO_4, this might provide clues for understanding the peculiar magnetoresistance behavior recently reported in Sr_2IrO_4[28]. The experiment by Ge *et al.*[28] seems to indicate a spin-flop-like transition upon application of the external fields parallel to the *c*-axis. This implies a possible switching of the magnetic configuration by external fields and a significant change of the electronic structure in Sr_2IrO_4. Our results also suggest a possible insulator-to-metal transition driven by external magnetic field in the epitaxially strained SIO superlattices and ultrathin films.

Fig. 3(d) shows the change of spin moments with respect to strain. While the spin moment is reduced by increasing tensile strains in the canted AF phase, it is enhanced in the collinear AF state. This feature can be understood by considering the strain-induced tetragonal crystal fields and the low-energy states which have deviated from the ideal $j_{\rm eff}$=1/2 as follows. Let us consider the t_{2g} states with the dominating SOC, λ, and the nonvanishing tetragonal fields, $\Delta_{\rm t}$. The effective atomic Hamiltonian is

$$\mathcal{H}_{\rm eff} = \lambda \mathbf{l}_{\rm eff} \cdot \mathbf{s} + \Delta_{\rm t} l^2_{{\rm eff},z}, \tag{2}$$

where $\lambda < 0$ for the t_{2g} states. Among the six eigenstates of Eq. (2), the upper twofold-degenerate states are given by[31]

$$|\widetilde{\pm}\rangle_z = \pm \sin\theta |0,\uparrow\downarrow\rangle_z \mp \cos\theta |\pm 1,\downarrow\uparrow\rangle_z, \tag{3}$$

or, when quantized along the in-plane (say, the octahedral x-direction),

$$|\widetilde{\pm}\rangle_x = 1/\sqrt{2}(|\widetilde{+}\rangle_z \pm |\widetilde{-}\rangle_z). \tag{4}$$

The orbital angle θ is defined as $\tan(2\theta) = 2\sqrt{2}\lambda/(\lambda - 2\Delta_{\rm t})$, and in the perfect cubic symmetry ($\Delta_{\rm t} = 0$, $\theta_{\rm cubic} \simeq 0.2\pi$) Eq. (3) reduces to the ideal $j_{\rm eff} = 1/2$ states defined in Eq. (1). From Eq. (2) one can notice that the presence of the tensile strain or the confinement effect, which lowers the energy of the d_{xy} state ($\Delta_{\rm t} > 0$), corresponds to the smaller θ. The strain dependence of the ordered spin moment in the collinear and the canted AF phases can be estimated from Eq. (3) and (4), respectively. For the collinear AF, $|\widetilde{\pm}\rangle_z$ forms the lower/upper Hubbard bands to yield the local spin and orbital moments parallel to the z-axis on the Ir sites. The expectation value of s_z is

$$\langle\widetilde{\pm}|s_z|\widetilde{\pm}\rangle_z = \mp 1/2\cos(2\theta). \tag{5}$$

In the canted AF phase, on the other hand, the moments are parallel to the octahedral x-axis, and the expectation value is

$$\langle\widetilde{\pm}|s_x|\widetilde{\pm}\rangle_x = \mp 1/4(1 - \cos(2\theta)). \tag{6}$$

It is clear that $|\langle\widetilde{\pm}|s_z|\widetilde{\pm}\rangle_z|$ and $|\langle\widetilde{\pm}|s_x|\widetilde{\pm}\rangle_x|$ behave in different ways with respect to $\Delta_{\rm t}$; with larger tensile strains, $|\langle\widetilde{\pm}|s_z|\widetilde{\pm}\rangle_z|$ is enhanced and $|\langle\widetilde{\pm}|s_x|\widetilde{\pm}\rangle_x|$ is reduced. This is consistent with the results of Fig. 3(d) in the region $\theta < \pi/4$. Since the confinement effect in the SL introduces a significant amount of $\Delta_{\rm t} > 0$, the θ is smaller than $\theta_{\rm cubic} < \pi/4$ over the entire range of strains.

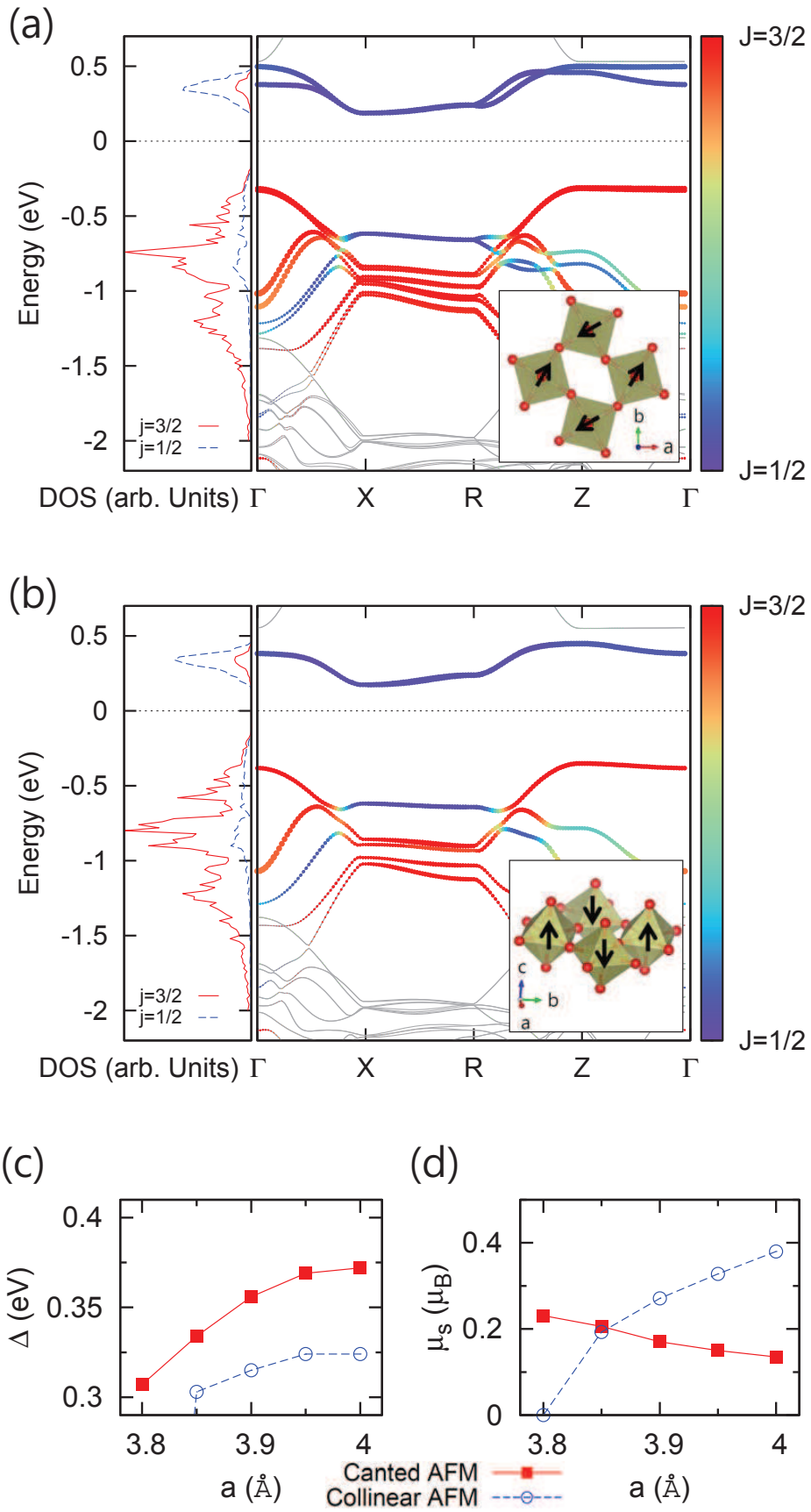

FIG. 3: The calculatd band structure calculated with SOC and U_{eff}=2 eV ($a = 3.95$ Å) for (a) the canted AF and (b) collinear AF order. The calculated (c) band gap Δ and (d) spin magnetic moment as a function of the in-plain lattice constant.

IV. CONCLUDING REMARKS

We have investigated the structural, electronic, and magnetic properties of SIO/STO SL. The results clearly demonstrate the similarity between $[SIO]_1$ /$[STO]_1$ SL and bulk Sr_2IrO_4, as expected from their structural similarities. By adding extra dimensions of controllability, the SL form of iridates can provide interesting new information for understanding the 5*d* transition metal oxides. It can be an important next step to investigate $[SIO]_2/[STO]_{n\geq 1}$ in comparison with $Sr_3Ir_2O_7$[25,29]. As the SIO-layer thickness is increased from the ultrathin limit to the bulk regime, the electronic structure can evolve from the insulating to the nodal semimetallic phase which also deserves intensive future study[14,26,30].

Acknowledgements

We thank Sung Seok (Ambrose) Seo, Hosub Jin, and Jaejun Yu for helpful discussion. This research was supported by Basic Science Research Program through the National Research Foundation of Korea(NRF) funded by the Ministry of Education(Grant No. 2013R1A6A3A01064947). Computational resources were provided by the National Institute of Supercomputing and Networking/Korea Institute of Science and Technology Information with supercomputing resources including technical support (Grant No. KSC-2013-C2-024).

References

* Electronic address: mj.han@kaist.ac.kr

[1] Datta S and Das B 1990 *Appl. Phys. Lett.* **56** 665
[2] Qi X-L, Li R, Zang J and Zhang S-C 2009 *Science* **323** 1184
[3] Mattheiss L F 1976 *Phys. Rev. B* **13** 2433
[4] Kim B J, Jin H, Moon S J, Kim J Y, Park B-G, Leem C S, Yu J, Noh T W, Kim C, Oh S J, Park J-H, Durairaj V, Cao G and Rotenberg E 2008 *Phys. Rev. Lett.* **101** 076402
[5] Kim B J, Ohsumi H, Komesu T, Sakai S, Morita T, Takagi H and Arima T 2009 *Science* **323** 1329
[6] Witczak-Krempa W, Chen G, Kim Y B and Balents L (2013) arXiv:1305.2193
[7] Kane C L and Mele E J 2005 *Phys. Rev. Lett.* **95** 226801
[8] Chang C-Z, Zhang J, Feng X, Shen J, Zhang Z, Guo M, Li K, Ou Y, Wei P, Wang L-L, Ji Z-Q, Feng Y, Ji S, Chen X, Jia J, Dai X, Fang Z, Zhang S-C, He K, Wang Y, Lu L, Ma X-C and Xue Q-K 2013 *Science* **340** 167
[9] Shitade A, Katsura H, Kuneš J, Qi X-L, Zhang S-C and Nagaosa N 2009 *Phys. Rev. Lett.* **102** 256403
[10] Rayan Serrao C, Jian Liu, Heron J T, Singh-Bhalla G, Yadav A, Suresha S J, Paull R J, Yi D, Chu J H, Trassin M, Vishwanath A, Arenholz E, Frontera C, Železný J, Jungwirth T, Marti X and Ramesh R 2013 *Phys. Rev. B* **87** 085121
[11] Nichols J, Terzic J, Bittle E G, Korneta O B, De Long L E, Brill J W, Cao G and Seo S S A 2013 *Appl. Phys. Lett.* **102** 141908
[12] Nichols J, Korneta O B, Terzic J, De Long L E, Cao G, Brill J W and Seo S S A 2013 *Appl. Phys. Lett.* **103** 131910
[13] Jenderka M, Barzola-Quiquia J, Zhang Z, Frenzel H, Grundmann M and Lorenz M 2013 *Phys. Rev. B* **88** 045111
[14] Jobu Matsuno *et al.*, Indo-Japan conference on New functionalities in electronic and magnetic materials (Bangalore, OCTOBER 2012); Workshop on Oxide Electronics 20 presentation (Singapore, September 2013).
[15] Han M, Ozaki T and Yu J 2006 *Phys. Rev. B* **73** 045110
[16] http://www.openmx-square.org
[17] Ozaki T 2003 *Phys. Rev. B* **67** 155108
[18] Perdew J P, Burke K and Ernzerhof M 1996 *Phys. Rev. Lett.* **77** 3865
[19] Dudarev S L, Botton G A, Savrasov S Y, Humphreys C J and Sutton A P 1998 *Phys. Rev. B* **57** 1505
[20] Arita R, Kuneš J, Kozhevnikov A V, Eguiluz A G and Imada M 2012 *Phys. Rev. Lett.* **108** 086403
[21] Foyevtsova K, Jeschke H O, Mazin I I, Khomskii D I and Valenti R 2013 *Phys. Rev. B* **88** 035107
[22] Kresse G and Hafner J 1993 *Phys. Rev. B* **47** 558
[23] Kresse G and Furthmüller J 1996 *Phys. Rev. B* **54** 11169
[24] Crawford M K, Subramanian M A and Harlow R L 1994 *Phys. Rev. B* **49** 9198
[25] Zhang H, Haule K and Vanderbilt D 2013 *Phys. Rev. Lett.* **111** 246402
[26] Moon S J, Jin H, Choi W S, Lee J S, Seo S S A, Yu J, Cao G, Noh T W and Lee Y S 2009 *Phys. Rev. B* **80** 195110
[27] Jin H, Jeong H, Ozaki T and Yu J 2009 *Phys. Rev. B* **80** 075112
[28] Ge M, Qi T F, Korneta O B, De Long D E, Schlottmann P, Crummett W P and G. Cao 2011 *Phys. Rev. B* **84** 100402(R)

[29] Kim J W, Choi Y, Kim J, Mitchell J F, Jackeli G, Daghofer M, van den Brink J, Khaliullin G and Kim B J 2012 *Phys. Rev. Lett.* **109** 037204
[30] Carter J-M, Vijay Shankar V, Ahsan Zeb M and Kee H-Y 2012 *Phys. Rev. B* **85** 115105
[31] Jackeli G and Khaliullin G 2009 *Phys. Rev. Lett.* **102** 017205